Noname manuscript No.
(will be inserted by the editor)

Determination of ice content in hardened concrete by low temperature calorimetry: influence of baseline calculation and heat of fusion of confined water

Min Wu · Björn Johannesson · Mette Geiker

Received: date / Accepted: date

Abstract Low temperature calorimetry (LTC) has been used to determine the ice content in concrete at different temperatures when exposed to low temperature environments. However, the analysis of the ice content from the measured data of heat flow is not straightforward. In this study, two important factors influencing the ice content calculation are discussed. The importance of the baseline determination for the calculation of the ice content is realized. Two different methods of generating the baseline are discussed. Firstly, the 'J-baseline' is discussed which is a recently proposed extrapolation method based on the accumulated heat curves measured in the freezing and the melting process. Secondly, the 'C-baseline' is discussed in which a calculated baseline is used where the heat capacity of both water and ice and the phase changing behavior under different testing temperatures are considered. It turns out that both the 'J-baseline' method and the 'C-baseline' method can be used to calculate the approximate baseline. The heat of fusion of the water confined in small pores is another important parameter to be considered in ice content calculation. This property must be carefully analyzed in order to accurately calculate the ice contents at different temperatures in the freezing and melting process. It should be noted that there is no general agreement on how to obtain the important temperature dependence of the heat of fusion of water confined in small pores. By performing comparison studies, the present study shows the influence of the different values of the heat of fusion commonly adopted on the calculated ice content for the studied concrete samples. The importance and necessity to use an accurate value of the heat of fusion is emphasized. Based on the calculation of the baseline proposed in this work and by carefully selecting the values for the heat of fusion, the ice content in a hardened concrete sample is expected to be estimated with an acceptable accuracy.

Keywords Low temperature calorimetry (LTC), Ice formation, Baseline calculation, Heat of fusion, Thermoporometry, Cryoporometry

Min Wu · Björn Johannesson
Department of Civil Engineering, Building 118
Technical University of Denmark, 2800 Lyngby, Denmark
E-mail: miwu@byg.dtu.dk

Mette Geiker
Department of Structural Engineering,
Norwegian University of Science and Technology, Trondheim, Norway

1 Introduction

Concrete is the most widely used construction material. As many structures have requirements to a long service life, durability is given special emphasis. In cold regions, the degradation of concrete is, among other reasons, often related to the freeze/thaw resistance (the resistance against frost damage). Concrete itself is a porous material with a rather complicated pore system, whose pore sizes can range from nanometer to millimeter [1, 2]. Due to the confinement of pores with different sizes, water present in the pores of concrete freezes at different temperatures when it is exposed to low temperature environments. The amount of ice formed in concrete at low temperatures is an important property when studying the freeze/thaw durability [3].

Low temperature (micro-)calorimetry (LTC), which is also known as thermoporosimetry and sometimes is referred to as thermoporometry or cryoporometry [4], can be used to determine the ice content in concrete at different temperatures by carefully studying the freezing/melting behavior of the confined water in the pores. The basic concept is that freezing of water is an exothermic process and the melting of ice is an endothermic process. The LTC instrument (calorimeter) records the heat flow of the sample at different testing temperatures. By analyzing the heat flow due to ice formation or melting at each temperature, the ice content in the freezing and melting process can be calculated by using the heat of fusion of the confined water/ice.

In addition to the determination of ice content, LTC is often adopted as a method to study the porosity of a material. Porosity characterization by using the measured freezing/melting temperature shift of a liquid, with which the porous material is saturated, was pioneered by researchers in a study of organic gels as early as 1950s [5]. The method was generalized and has been applied to different materials, e.g., inorganic materials [6], organic materials [7–10], soil [11] and cement based materials [4, 12], etc. A detailed description of the thermodynamic basis for the derivation of the pore size distribution based on LTC measurement is attributed to Brun et al. [13]. By considering the thermodynamics, it shows that there is a unique relation between the triple point temperature of the probe liquid confined in the pores of a material and the curvature of the solid-liquid interface. Thus, by using the thermodynamic parameters of the probe liquid, i.e., surface tension, heat capacity and heat of fusion, the approximate relation between the freezing/melting temperature and the pore size can be quantified. Water is commonly chosen as a probe liquid. The advantage of using water as the probe liquid is two fold. Firstly, water is a well studied substance implying that the standard thermodynamic parameters are well documented; secondly, the specific heat capacity of water is much larger compared with that of other liquids, especially organic solutions. Thus, the measured heat flow during the freezing or melting process is comparably large and even a small amount of water undergoing phase change can be detected and recorded by the LTC instrument. However, for the determination of pore size distribution for cement based materials, additional information is needed. For example, the solidification mechanism of the water confined in small pores must be constituted by suitable assumptions. Different assumptions about the solidification mechanisms of confined water are discussed, e.g., in [13–17]. The concept of un-freezable layer of water (or $\delta-$layer) is introduced in [12, 13] and the effect of ion concentrations in the pore solution is discussed in [4, 12, 18]. It should also be mentioned that in the context of using LTC to determine pore size distribution, the thermodynamic relation between pore size and the depressed phase change temperature is often derived based on the prerequisite that the pores under study are fully saturated. That is, there is only one interface, i.e., the solid-liquid interface, in the pore system. If the pores under consideration are not fully saturated, more interfaces could exist (i.e., the vapor-liquid and the vapor-solid interface) and there are several possibilities with respect to the coexistence of the interfaces, e.g., see [6, 12, 13, 19, 20], which makes the quantitative determination of the relation between pore size and the depressed phase change temperature extremely difficult. This is of particular relevance for air-entrained cement based materials, in which proper care should be taken to ensure fully saturation. The impact of sample saturation on the detected porosity of hardened concrete is discussed in a relatively detailed manner in [21]. Further discussions of related aspects fall outside the scope of this paper.

The study of ice formation in cement based materials dates back to early 1970s [12, 22, 23]. Systematic study of cement based materials using LTC was initiated in early 1980s [24, 25], in which some fundamentals for the application of the method, including the test procedures, ice calculation method and the heat of fusion of pore confined water *versus* temperature, were explored. Following that, LTC was used to investigate important aspects of cement based materials, e.g., the stability of the materials to temperature and drying treatment [26–28], effects of supplementary materials on the pore structure of the materials [25, 29, 30]. Other relevant studies in this regard include, e.g., [31, 32].

Although LTC has been adopted to determine the ice content in cement and concrete materials for several decades, there are some aspects that need to be further addressed. The heat flow measured by a LTC instrument at each time consists of two parts: (1) the contribution from the heat capacity of the system (including water and ice in the concrete sample, and also the concrete skeleton matrix), which will be mentioned as the "heat flow baseline" or simply "baseline" in our discussion; and (2) the contribution due to phase transition. In order to calculate the ice content, one needs to know how much energy goes to form or melt ice at each temperature level under consideration, indicating that the baseline should be determined. During each test, the ice in the pores of the concrete will be continuously forming/melting as the temperatures decreases/increases (due to the relative wide distribution of the pores in concrete), which means that the baseline of the heat flow is continuously changing due to the change in the proportion of ice and liquid water confined in the pores. What makes it even more difficult to determine the baseline is that the heat capacities of water, ice and the solid matrix are temperature dependent. Moreover, the water under study in this case is the water confined in very small pores. Although bulk water is a well studied substance, some of the thermodynamic parameters, e.g., heat of fusion, of the confined water and ice still need to be further investigated.

It should be noted that LTC is not a straightforward method since: (1) the measurement provides information on the overall apparent heat capacity of the sample at different temperatures, not only that due to the water/ice phase transition; and (2) the heat of fusion of the confined water/ice needs to be known beforehand since this method itself cannot measure the temperature dependence of the heat of fusion. This study focuses on the calculation of ice content from measured data of heat flow by a LTC instrument. Comparison studies will be performed to demonstrate the impact of two different ways of calculating baseline and the different values of heat of fusion for confined water commonly adopted in literature on the calculated ice content.

2 Experimental data

This investigation is based on existing experimental data on micro-concrete samples with three different water-to-cement ratios (w/c=0.4, 0.5 and 0.6) and different target air contents of 2%, 4% and 6%[1]. The details of the experimental study are presented in [33–35].

The cement content for the w/c=0.4 concrete samples with target air contents of 2%, 4% and 6% were 515, 525 and 525 kg m^{-3}, respectively. And the corresponding values for the w/c=0.5 and w/c=0.6 samples were 475, 480 and 480 kg m^{-3} and 340, 350 and 335 kg m^{-3}. Approximately equal amount of granite aggregate with two different size ranges, i.e., 0-3 mm and 4-8 mm, were used to prepare all the mixes. The samples were produced in 120 L batches in the laboratory. After mixing, the fresh concrete was placed into moulds. The moulds filled with fresh concrete were vibrated for a few seconds before a plastic film was placed on top to prevent evaporation. After curing under sealed condition for one day, the micro-concrete cylinders used in the calorimetric measurements were core-drilled and sawn into small cylinders with the diameter of 14 mm and the length of 60 mm. The size of the samples was chosen to fit the calorimetric device used in the investigation. Based on visual inspection it was concluded that no damage of samples was introduced by the early drilling

[1] In concrete technology, the freeze/thaw resistance of concrete can be improved by entraining a certain amount of high quality air voids, typically 4-6 vol%, e.g., see [3].

and sawing. The samples were stored in water at about 20 °C for about four months before testing (mentioned as capillary saturated samples).

A Calvet-type scanning calorimeter (SETARAM) was used for this investigation, which was calibrated and operated to work between about 20 °C and -130 °C. The temperature scanning consisted of a cycle starting at 20 °C and going down to about -80 °C and then back to 20 °C. The adopted cooling and heating rate was 5.4 °C h^{-1}. The samples were saturated surface dry when placed in the calorimeter. A totally dried concrete sample, of the same dimensions as the samples, was used as the reference sample in the calorimetric measurements. The same reference sample was used throughout the investigation. By using this type of reference sample, it was possible to simplify the calibration of the measurement. During the testing, the calorimeter records the calibrated heat supplied to or released from the sample. This means that the instrument measures the difference of the heat flow between the reference and the sample chamber, thus the overall heat flow response due to the confined pore water and its phase change in a sample at different temperatures can be determined. At the same time, the corresponding temperature of the sample chamber is also recorded.

The procedures of calorimetric measurements performed here differ from the "old" ones as adopted in, e.g., [4, 28], mainly by two aspects: (1) the cooling and heating rate adopted in this work were slightly higher (which were 3.3 °C h^{-1} and 4.1 °C h^{-1}, respectively, in the "old" procedures); (2) AgI was used as a nucleation agent in the "old" procedures, while it was not used in this work. It is noted that in literature, there is no general agreement on the cooling and heating rate and they vary quite a lot, e.g., from about 15 °C min^{-1} to 1 °C h^{-1} [36]. The study on concrete samples [20] showed that the cooling/heating rate between 3 and about 8 °C h^{-1} does not have an important impact on the measured heat flow and further the calculated ice content. Of this reason we think that the cooling/heating rate used in this work would have little impact on the ice content calculation compared with the "old" procedures. The use of AgI helps to reduce supercooling effect. A typical water saturated concrete sample without AgI freezes at about -8 or -9 °C [33] while it could be reduced to about -4 or -5 °C by using AgI [4]. On the other hand, the added AgI may enter into the pore water, which could possibly complicate the analysis of the freezing behavior, e.g., affecting the freezing point and the heat of fusion, etc. Since adding AgI does not completely cancel out the supercooling effect and it may complicate the analysis of the data, it was not added in this work.

After a calorimetric measurement, the sample was dried under about 105 °C till constant weight. By doing so, the total water content of the sample was determined by the mass difference between this dried state and that before the calorimetric measurement (saturated surface dry).

More detailed explanations about the sample preparation and calorimetric measurements can be found in [33].

3 Interpretation of the measurement results

3.1 Baseline and ice content calculation

As discussed in Introduction, in order to calculate the ice content, the baseline of the heat flow need to be determined. The baseline will be continuously changing during the water/ice phase transition. This is among other things due to that the heat capacity of water is about twice as large as that of the ice (e.g., compare Eq.3 with Eq.4). Therefore, the baseline will be moved upwards when ice transforms into water and downwards when water changes into ice, with the magnitude depending on the involved amount of water/ice undergone phase transition. The difficulty of calculating the baseline in an exact manner is due to the continuously changing proportion of ice and water and the dependency of the heat capacities of water, ice and the concrete skeleton matrix on the temperature. This is especially true when the temperature in testing covers a large range. In the following discussion, two methods of calculating the baseline and the ice content will be presented.

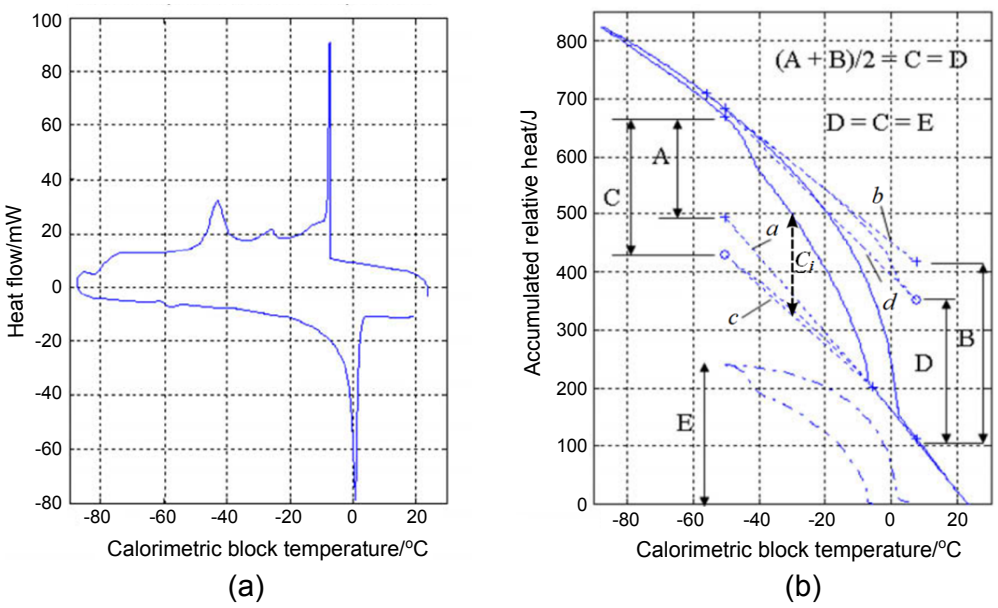

Fig. 1: An example showing how to construct the baseline using 'J-method'. (a) measured heat flow data from the calorimeter; (b) integrated values of heat responses (solid line) and data treatment to achieve a proper baseline (adapted from [33]).

3.1.1 'J-baseline' method

A detailed explanation of the original 'J-baseline' method is presented and discussed in [33]. Initially, the measured heat flow curves are corrected assuming a closed system, i.e., the heat developed during freezing corresponds to the heat loss during melting. After the initial calibration, the accumulated heat is integrated and shown as the solid line in Figure 1b, from the corrected heat flow curve as shown in Figure 1a. The first step in the analysis of the integrated heat curves according to Figure 1b, concerns the extrapolation of the initial total heat capacity of the system before freezing starts, which is shown in the curve denoted by *a* in Figure 1b. The extrapolated heat capacity for the same system when all of the ice has been formed can be constructed in the similar manner. Hence, the curve denoted by *b* as shown in Figure 1b can be constructed. The energy jump denoted by A in Figure 1b is the accumulated heat difference between the extrapolated fictive energy level, given by the curve *a*, and the measured total accumulated energy level at the end of the active ice forming stage (when the accumulated heat curve becomes linear). Similarly, the energy jump denoted by B is the heat difference between the extrapolated fictive energy level as given by the curve *b* and the true measured total accumulated energy level at the time when all of the ice is melted. It is concluded that the energy jump A is an underestimated value compared with the true energy jump caused by the solidification energy involving the formation of ice. This is because ice is continuously formed during the freezing process which will result in a continuous decrease of the baseline as more ice is formed. The decrease of the baseline is not reflected in the extrapolated baseline associated with the curve *a*. In a similar manner, the energy jump from the frozen stage to the stage when all ice is melted given by the 'distance' B in Figure 1b, overestimates the total fusion energy for the melting process.

Based on the above discussion, it is realized that the true total required energy to convert all water to ice or *vice versa* must lie somewhere in between the values indicated by the 'distances' A and B in Fig 1b. By adopting an explicit and somewhat crude assumption that the total required energy to convert all water to ice or *vice versa* of the sample is the average value of A and B, i.e., (A

+ B)/2, a baseline can be constructed. This assumption was checked for its performance by running a calorimetric test from room temperature to about -20 °C using pure water in [20]. The results in the verification testing show a deviation about 2% of the tabulated heat of fusion of ice. For this reason, it is assumed that the adopted direct method performs in a manner which is acceptable. It should be remarked, however, that this type of verification does not include the varying freezing temperatures of water due to the pore confinement.

The average value of the energy jumps C = D defined by A and B, as shown in Figure 1b, is used to determine new endpoints (marked with circles on the curves denoted by c and d). The next step in the procedure consists of making a non-linear weighting between the extreme curves a and c during the freezing process and between the extreme curves b and d during the melting process. The non-linear weighting is conducted like this: at any temperature (taking the freezing as an example), the "distance" between the accumulated heat curve and the true baseline is calculated as the "distance" between the accumulated heat curve and the curve c, denoted as C_i in Figure 1b, multiplying by a factor of C_i /C. The same procedure is also applied to the melting curves. The two obtained weighted curves, i.e., the ones lying in between the curves a and c and in between b and d, are used as the baselines for the experiment from which the accumulated energy with respect to the ice formation can be determined. The obtained curves for accumulated energy during the ice formation and melting are also shown in the lower part of Figure 1b. The ice content corresponding to each temperature can be calculated through dividing the accumulated heat by the heat of fusion of the confined water/ice.

It has been reported in many studies, e.g., in [7, 13, 18, 36–39], that there is a hysteresis behavior in terms of ice content curves in the freezing and melting process, indicating that for the ice confined in the same pores, the ice formation temperature could be different from its melting temperature. As will be discussed later in Section 3.2, the heat of fusion of the confined water/ice could be a temperature dependent property. Consequently, in one measurement cycle consisting of a freezing and a melting process, the accumulated heat released in the freezing process is not necessarily equal to the heat absorbed in the melting process. Thus, the measured heat flow is not necessarily a closed system. It turns out that the initial calibration of the heat flow by assuming it is a closed system is not necessarily relevant. However, it should be noted that the maximum ice content formed in the freezing process should be equal to that melted in the melting process in one measuring cycle (mass conservation). By keeping this in mind, the curves of the accumulated energy can be further tuned by making additional assumptions concerning the temperature dependence of the heat of fusion (Section 3.2) in order to give an estimate of the ice contents at different freezing and melting temperatures. The tuning is conducted by decreasing the slope of line a and increasing that of b with the same percentage (referring to Figure 1b) if the ice calculated in the freezing is less than that in melting, and the other way around. The purpose of doing this further tuning is to ensure that the ice content determined from the freezing process is exactly the same as that from the melting process.

3.1.2 'C-baseline' method

As can be seen from the above discussion, the 'J-baseline' determination is an extrapolating process based on certain assumptions. Alternatively, it is possible to calculate the baseline and the ice content based on the heat capacities of ice and water by taking into account the phase changing behavior of the confined water or ice in a sample under different temperatures in a test. The method has more theoretic basis and it will be mentioned as 'C-baseline' method in the following discussion. The 'C-baseline' method presented here is originated from a method established by Sun and Scherer in [18] with slight modification.

Before further discussion, a clarification should be made about the pore liquid in the concrete samples under this study. Actually, the liquid confined in the pores of concrete samples is not pure water, which contains certain ionic species [40, 41]. However, the pore liquid will be simply assumed as pure water first and the possible effect of the ions on the calculated results will be discussed later in Section 4.

The measured heat flow consists of two parts, the baseline and the heat flow due to phase transition. The baseline comprises the heat capacity of the whole system, including pore water and ice as well as the concrete skeleton matrix if no reference sample is used. The experimental data discussed in this paper were obtained using a reference sample of dried concrete with the same size as the samples tested, and we assume the concrete skeleton matrix has no influence on the measured heat flow. Thus, the overall heat capacity of the system contributed to the baseline in our testing is only attributed to the water and ice in the concrete sample. a more discussion about the reference sample will be presented later.

The total heat flow into or out of a sample measured by the LTC instrument at any time is denoted by Q, while the baseline and the heat flow due to the phase transition at any time are denoted by Q_B and Q_S, respectively. Thus we have $Q = Q_B + Q_S$. If h is used to denote the heat of the sample (not including the contribution from the phase transition) and t is the time, we have $Q_B = dh/dt$. The cooling or heating rate in the testing is q and T is the temperature, then $q = dT/dt$. Accordingly, the overall heat capacity of the system at any time C_p can be derived and expressed as

$$mC_p = \frac{dh}{dT} = \frac{dh}{dt} \cdot \frac{dt}{dT} = \frac{Q_B}{q} \tag{1}$$

where m is the total mass of the confined water and ice in the sample. In terms of the cooling/heating rate q, it should be noted though it is often set at a constant value during a measurement, while there is always certain degree of drifting or fluctuation, big or small. As shown in Eq.1, the baseline Q_B is depending on the cooling/heating rate q, which means the drifting or fluctuation of q will affect the measured Q_B and thus the measured overall heat flow Q. Thus, it makes more sense to take into account this measured q in a testing, rather than the set constant value, especially when some important fluctuations occur. As already mentioned, since a dry sample is used in the reference chamber of the LTC instrument, the overall heat capacity is due to liquid water and ice confined in the pores of the sample, thus we have Eq.2, where m_l is the mass of pore water and m_s is the mass of the formed ice, C_{pl} and C_{ps} are the heat capacity of water and ice, respectively.

$$mC_p = m_l C_{pl} + m_s C_{ps} \tag{2}$$

The heat capacity of water and ice are assumed to be not very sensitive to temperature according to [42, 43], as shown in Eq.3 and Eq.4, where θ is the temperature in °C. So an approximation is made by treating them as constant without resulting in major errors. It is also noted that different temperature dependence about the heat capacity of water and ice are reported, e.g., in [44]. More related discussions will be conducted later.

$$C_{pl} = 4.222\left(1 - 54 \cdot 10^{-5}\theta\right) \qquad \text{J g}^{-1}\text{K}^{-1} \tag{3}$$

$$C_{ps} = 2.114\left(1 + 373.7 \cdot 10^{-5}\theta\right) \qquad \text{J g}^{-1}\text{K}^{-1} \tag{4}$$

Nevertheless, this approximation enables us to differentiate Eq.2 analytically. If the initial mass of the pore liquid is m_{l0}, we have $m_l = m_{l0} - m_s$. Thus, the change in the heat capacity is clearly related to the change of the mass of ice, as shown in Eq.5.

$$m\frac{dC_p}{dt} = (C_{ps} - C_{pl})\frac{dm_s}{dt} \tag{5}$$

Just before the water starts to freeze (right before the first peak observed on a measured heat flow curve during freezing), the heat flow is denoted as Q_0 and the corresponding cooling/heating rate and the time are denoted as q_0 and t_0, then

$$Q_0 = q_0 m C_{p0} = q_0 m C_{pl} \tag{6}$$

The changing of the heat capacity of the system can be related to the change of the ice mass by integrating Eq.5. The relation is shown in Eq.7.

$$m\left(C_p(t) - C_p(t_0)\right) = (C_{ps} - C_{pl})m_s \tag{7}$$

By multiplying both sides of Eq.7 by $q(t)$ and inserting Eq.6, Eq.9 can be obtained, where $Q_B(t)$ is the baseline at any proceeding time after t_0.

$$q(t) \cdot m\left(C_p(t) - C_p(t_0)\right) = q(t) \cdot (C_{ps} - C_{pl})m_s \tag{8}$$

$$Q_B(t) - Q_0\frac{q(t)}{q_0} = q(t) \cdot (C_{ps} - C_{pl})m_s \tag{9}$$

Thus, $Q_B(t)$ can be obtained by rearranging Eq.9, which is

$$Q_B(t) = q(t) \cdot \left(\frac{Q_0}{q_0} + (C_{ps} - C_{pl})m_s\right) \tag{10}$$

The heat flow due to phase transition is given in Eq.11, where Δh is the heat of fusion of the confined water or ice, m_s is the mass of the ice in the pores of the sample tested. As mentioned earlier, different arguments exist with respect to the determination of heat of fusion for the confined water in the freezing and melting process. Brun et al. [13] proposed that unlike the bulk water, the heat of fusion for the water confined in pores in the freezing process will be different from that in the melting process for cases in which cylindrical pore shape is assumed. The details will be further explored in the next section. Here, it should be noted that the heat of fusion in the freezing and the melting processes may differ. By using Δh_f (in freezing) or Δh_m (in melting) in the place of Δh, Eq.11 describes the case for freezing or melting respectively.

$$Q_s(t) = \Delta h\frac{dm_s}{dt} \tag{11}$$

As mentioned before, the total measured heat flow $Q(t)$ is the sum of the baseline and the heat flow due to phase transition, which leads to the conclusion that

$$Q(t) = Q_B(t) + Q_s(t) = q(t) \cdot \left(\frac{Q_0}{q_0} + (C_{ps} - C_{pl})m_s\right) + \Delta h\frac{dm_s}{dt} \tag{12}$$

Then, Eq.12 is rearranged to give

$$\frac{dm_s}{dt} + \frac{q(t) \cdot (C_{ps} - C_{pl})}{\Delta h}m_s = \frac{Q(t) - Q_0 \cdot q(t)/q_0}{\Delta h} \tag{13}$$

In a measurement, the LTC instrument will record the heat flow and the corresponding temperature of the sample chamber continuously. Thus in Eq.12, $Q(t)$ will be given directly by the LTC instrument and $q(t)$ can be obtained by dividing the measured temperature gradient by the time interval in the calculation step. The heat of fusion Δh will be determined as an input, which will be described in the next section. So, there is only one unknown m_s. By solving Eq.13 numerically, we will obtain the ice content at each time (corresponding to each temperature) accordingly.

It should be noted the baseline for the freezing and the melting processes almost always are found to be different, due to the hysteresis effect in the freezing and melting process as mentioned earlier. The calculation method is, however, independent of the hysteresis and therefore Eq.13 is applicable for both the freezing and the melting process. By using Δh_f in the position of Δh in Eq.13 and Q_0 representing the heat flow before ice starts to form, the mass of ice is obtained directly. As for the melting process, theoretically we could find a relatively stable region with a constant heat flow Q_0 before the ice starts to melt. However, it is in practice difficult to determine the heat flow at that temperature. There are two reasons for this: firstly, the formed ice will be continuously melting and

the amount of the ice melted at low temperatures (approximately between -40 °C and -50 °C) is very small, if there is any; secondly, possible fluctuation of the heating rate could lead to the variations of the heat flow. A possible solution is to analyze the melting process inversely from the high to the low temperature end and treat the data similarly to a 'freezing process'. The Q_0 would then be the heat flow after all of the ice has been melted, see the melting curve in Figure 1a, which could be easily determined. By treating the melting process as a freezing process and using Δh_m in the position of Δh in Eq.13 combined with the determined Q_0, we can also calculate the ice content corresponding to each melting temperature.

The derivations performed here are slightly different from that conducted in [18], i.e., the possible drifting or fluctuation of the cooling or heating rate is included in this study (Eq.13). Comparison study using many sets of data [45] shows that the calculated ice content curves could be incorrect if the drifting or fluctuation of the cooling or heating rate is not considered. It is also noted that this possible drifting or fluctuation could also be very specific to the employed instrument for measurements. Moreover, compared with the experimental setup in [18], there was a reference sample used when undertaking the measurements for this study [33]. Since no reference sample was used in the experiments reported in [18], the appropriate corrections concerning the heat contribution due to the solid matrix was used in the analysis of the measured data. The assumption used in [18] is that the heat capacity of the skeleton matrix is a constant or at least it is not sensitive to temperature variation. This may be valid for some solid materials. However, the heat capacity of a material in general may vary to a certain degree under different temperatures. This variation can be further reduced by using a reference sample as described in the experiment. Additionally, the effect due to the possible uncertainties of the solid skeleton material during the freezing and melting can also be minimized by using the reference sample.

3.2 Heat of fusion of confined water/ice for ice content calculation

It has been mentioned earlier that the heat of fusion of the confined water or ice is an important parameter in calculating the ice content. However, there is no general agreement on which value should be used. The value of the heat of fusion for water confined in pores used for the analysis of LTC data can be divided into two groups: (1) as that for bulk water, but corrected based on the depressed freezing/melting temperature of the confined water, see e.g., Ishikiriyama et al. [46–49]; (2) modified by taking into account important correction terms, i.e., the lowered pressure of the liquid water and the water-ice interface formation, e.g., see Brun et al. [13, 50].

Ishikiriyama and co-workers [46–49] conducted a series of investigations and it was concluded that it is reasonable to assume that the heat of fusion of the confined water is the same as that of bulk water but with the correction based on the freezing/melting point depression of the pore water due to confinement. The value of the heat of fusion was suggested to be fitted to a polynomial as, e.g., adopted by Randall [51, 52]. The fitted heat of fusion $\triangle h$ is a temperature dependent function, which is shown in Eq.14, where T is the temperature in Kelvin degree. As it was further pointed out in [52], the validity of Eq.14 was verified by using an accurate absolute calorimeter and the difference between Eq.14 and the more accurate theoretical value calculated from Kirchhoff's law was negligible. Also, Eq.14 is used as the heat of fusion for the confined water in other LTC studies [36, 53, 54]. In the work presented in [4, 12, 24, 25, 28, 55], where $\triangle h$ is expressed as a linear function of T, the absolute value of the heat of fusion used is only slightly different from the results of Eq.14, thus the different groups of work give the same results in all essential parts. The assumption used is that the heat of fusion in the freezing and in the melting process have the same temperature dependence, i.e.,

$$\triangle h = 334.1 + 2.119(T - 273.15) - 0.00783(T - 273.15)^2 \qquad \text{J g}^{-1} \tag{14}$$

$$\triangle h_f = \triangle h_m = \triangle h \tag{15}$$

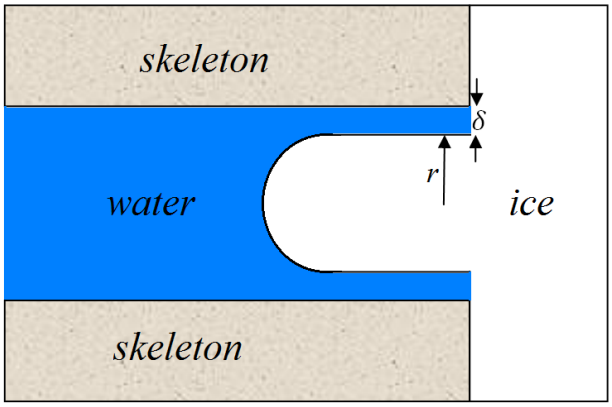

Fig. 2: According to Brun et al. [13, 50], there are two factors which influence the heat of fusion of the water confined in pores compared to its bulk state: (1) lowered pressure of the liquid water: due to that there is a layer of ice on the outer surface of the pores which is in equilibrium with its surrounding vapor (assumed), thus the liquid water confined in pores will be under negative pressure; (2) the water-ice interface formation.

where $\triangle h_f$ and $\triangle h_m$ is to denote the heat of fusion in freezing and melting, respectively.

Brun et al. [13, 50] proposed another procedure to derive the heat of fusion of confined water or ice and its temperature dependence. It was argued that external liquid water, and/or the possible water expelled from the sample during freezing, provides a layer of ice on the outer surface, which is in equilibrium with the surrounding vapor. If the solid ice remains in thermodynamic equilibrium with the atmosphere and with the liquid water in the pores, then the liquid water, as shown in Figure 2, must be under negative relative pressure. The pressure on the liquid water will affect the heat of fusion when it undergoes phase change. It is, further, argued by the same authors in [13, 50] that another correction term should also be added due to the formation of the solid-liquid interface in freezing and decomposition in melting. When ice forms in a pore, a solid-liquid interface is created. Thus, a portion of the energy is needed to form this ice-water interfacial surface. Accordingly, when the solid melts, the energy of this interface will be liberated. This portion of the liberated energy constitutes a positive contribution to the heat of fusion, whose magnitude depends on the surface area of the solid-liquid interface, or rather the radii of the pores where ice melts. A detailed derivation of this correction can be found in [50] and further discussion is conducted in [18].

By considering both the lowered pore pressure effect and the interfacial correction, the heat of fusion for water confined in pores in the freezing and the melting processes (mention as solidification and fusion energy in [13]) can be determined. The heat of fusion in freezing $\triangle h_f$ and the heat of fusion in melting $\triangle h_m$ as a function of temperature can be calculated from the definition of $\triangle h$, as shown in Eq.16, by using $(\Delta S_{sup})_f$ for the freezing process and $(\Delta S_{sup})_m$ for the melting process for ΔS_{sup} , respectively.

$$\Delta h = T\Delta S = T(\Delta S_f + \Delta S_{sup}) \tag{16}$$

where T is the temperature in Kelvin degree, ΔS is the overall entropy for the ice confined in pores, which consists of the solidification entropy ΔS_f and the interfacial entropy ΔS_{sup}. It is revealed that the correction terms due to the lowered pore pressure effect and the interface are important ones affecting the value of the heat of fusion [13]. Based on some simplifications, a theoretical calculation in the same paper demonstrates that in the freezing process, the effect of the lowered pressure of the pore water accounts for about 33% of the total decreased heat of fusion at -30 °C and the interfacial correction contributes about 25% increase to the heat of fusion when the temperature is -25 °C. By

inserting the numerical values generated from the assumptions and derivations performed in [13], the heat of fusion can be expressed in numerical terms. The modified heat of fusion in the freezing and the melting were then used in a series of their subsequent work [56–60] and also cited by other authors, e.g., [61–63].

Sun and Scherer [18] followed the same procedure as adopted by Brun et al. and calculated the heat of fusion. The results showed that the correction of the interfacial energy (corresponding to the formation of the solid-liquid interface) is an important factor in the freezing process, which almost offsets the temperature dependence of $\triangle h_f$. The corrected heat of fusion in the freezing was estimated as

$$\triangle h_f = 332.4 \qquad \text{J g}^{-1} \tag{17}$$

Following the approach adopted by Brun et al., the heat of fusion in melting process will be different compared with that of the freezing process. This is because the value of the interfacial correction depends on the curvature of the pores where ice melts. That is, the correction will be dependent on the assumption about the pore shape made. As argued in [13, 18], the curvature of the cylindrical pores with the same radius is only half as large as that in the freezing process and according to the calculation in [18], the corrected heat of fusion can be expressed as Eq.18 with very small relative error. While for spherical pores, since the curvature of pores with the same radius in freezing is the same as that in melting [13], Eq.17 works for both the freezing and the melting process [18].

$$\triangle h_m = 333.8 + 1.797(T - T_0) \qquad \text{J g}^{-1} \tag{18}$$

where T_0 is the melting point of bulk ice (freezing point of bulk water) in Kelvin degree.

According to the above discussion, it is noted that disagreement exists regarding how to obtain an expression for temperature dependence of the heat of fusion for the water or ice confined in pores. The temperature dependence of the heat of fusion by considering correction terms accounting for interfacial effects differ from that of the more simple bulk water assumptions and the difference becomes larger as the temperature decreases, especially for the freezing process. It is somehow difficult to judge which values for the heat of fusion of the confined water is more relevant in determining the ice content. Comparison studies will be conducted to show the difference of the calculated ice content based on the different adopted values of the heat of fusion for the confined water or ice.

4 Results and discussion

4.1 Ice content calculated based on the two different methods

The ice content was calculated for the different samples using the ‘J-baseline’ method and ‘C-baseline’ method described previously. The heat of fusion for bulk water/ice corrected for the depressed freezing/melting temperature, i.e., Eq.14, was used for the confined water or ice in the calculation using both ‘J-baseline’ method and ‘C-baseline’ method. The results for different samples are shown in Figure 3. According to the melting curves in Figure 3, it is noted there is a portion of ice which melts above 0 °C due to the lack of equilibrium between the sample and the instrument and maybe also inside of the sample, despite of the efforts being taken to avoid this. Compared with conventional LTC measurements in which the sample size is on the order of milligrams [7, 36], the samples used in this study are bigger. One may argue that the lack of equilibrium is probably due to the big sample size even if a very low cooling/heating rate is adopted. However, it is noted that a careful study by Landry [36] using 1-2 mg of water in conventional LTC experiments also found the extended melting above 0 °C. It should be mentioned that Riikonen et al. [7] discussed about the non-equilibrium issue and claimed that the sample during a typical LTC measurement is never in equilibrium state since it is measuring a dynamic process of freezing or melting.

Table 1: The maximum amount of ice by total water calculated from the freezing and melting process in one freezing and melting measurement cycle for the samples shown in Figure 3. The notation for the sample C404 means that w/c=0.40, target (nominal) air content 4%, and likewise.

Sample	J-baseline (%)	C-baseline (%)			Relative difference (%)[a]
		freezing	melting	average	
C404	39.7	32.7	32.4	32.6	17.9
C406	47.1	40.3	39.7	40.0	15.1
C504	48.5	41.8	43.6	42.7	11.9
C506	51.1	47.3	46.3	46.8	8.3
C602	55.9	49.9	50.4	50.2	10.2
C606	55.2	46.3	47.1	46.7	15.4

Note: (a). the relative difference is calculated by: 100(column 5-column 2)/column 2.

By studying the freezing curves, it is found that when the temperature decreases to about -50 °C, no more ice will be formed and there is still a certain proportion of water remained unfrozen in concrete samples as the temperature keeps decreasing. This is in agreement with the findings about mature concrete samples in [12, 24, 25, 33]. The shape of freezing curves based on 'J-baseline' and 'C-baseline' are quite similar and the ice contents calculated by the methods are in good agreement in the range of small temperature depressions. However, at larger temperature depressions, the difference between the ice content calculated by the two methods becomes bigger.

While for the melting curves as shown in Figure 3, the results based on the 'C-baseline' method show the ice confined in small pores starts to melt when the temperature reaches about -40 °C. This is somehow understandable if we compare the melting curve with the freezing curve. A plateau is found after about -50 °C in each of the freezing curves presented in Fig.3, implying no more ice formation even if the temperature further decreases. As demonstrated in many studies [13, 18, 34, 35, 47, 48], the freezing point of the water confined in pores with certain pore size is lower than the melting point of the ice confined in pores with the same pore radius. Possible reasons for this phenomenon include the pore shape effect, pore connectivity. Moreover, as pointed out earlier in some studies [13, 18, 61–63], in case of cylindrical pore shape, the depression of the freezing point could be as high as double the melting point depression. Thus, it is reasonable to believe that the ice formed at -50 °C will be melted at some temperature which is higher than -50 °C. The different starting points of the melting curves of the different concrete samples as shown in Fig. 3 could be related to the porosity of the samples, such as the pore volume, pore shape or the connectivity of pores. It is also found that the melting curve according to 'J-baseline' shows certain degree of agreement with that based on 'C-baseline' despite the difference becomes more obvious at the high depression range, i.e., the range of low temperatures. The maximum amount of ice formation calculated based on the two different methods are shown in Table 1. For the 'J-baseline' method, one of the principles is to ensure that the maximum ice formed in the freezing process is equal to ice melted in the melting process in one freezing and melting cycle, so we obtain the same value for the maximum ice content in the freezing and melting processes. While for the 'C-baseline' method, the ice content is calculated for the freezing and melting process respectively, thus we have different values of the ice content for the freezing and melting process. It is demonstrated that the maximum amount of the ice content determined for the freezing and melting process based on 'C-baseline' is very close to each other, giving a variation about less than 3%. It might imply the applicability of the method and Eq.14 as the heat of fusion of the confined water in this study. The issue about the heat of fusion for confined water will be further discussed in the next section. The maximum amount of ice determined based on 'J-baseline' and 'C-baseline' differs. For our study, the largest relative difference was found for the sample C404, which was as high as 18%; while the smallest relative difference was shown for the sample C506, which was about 8.5%.

Regarding the difference between the ice content calculated from 'J-baseline' method and 'C-baseline' method, possible explanations can be proposed if we look back into the calculation methods.

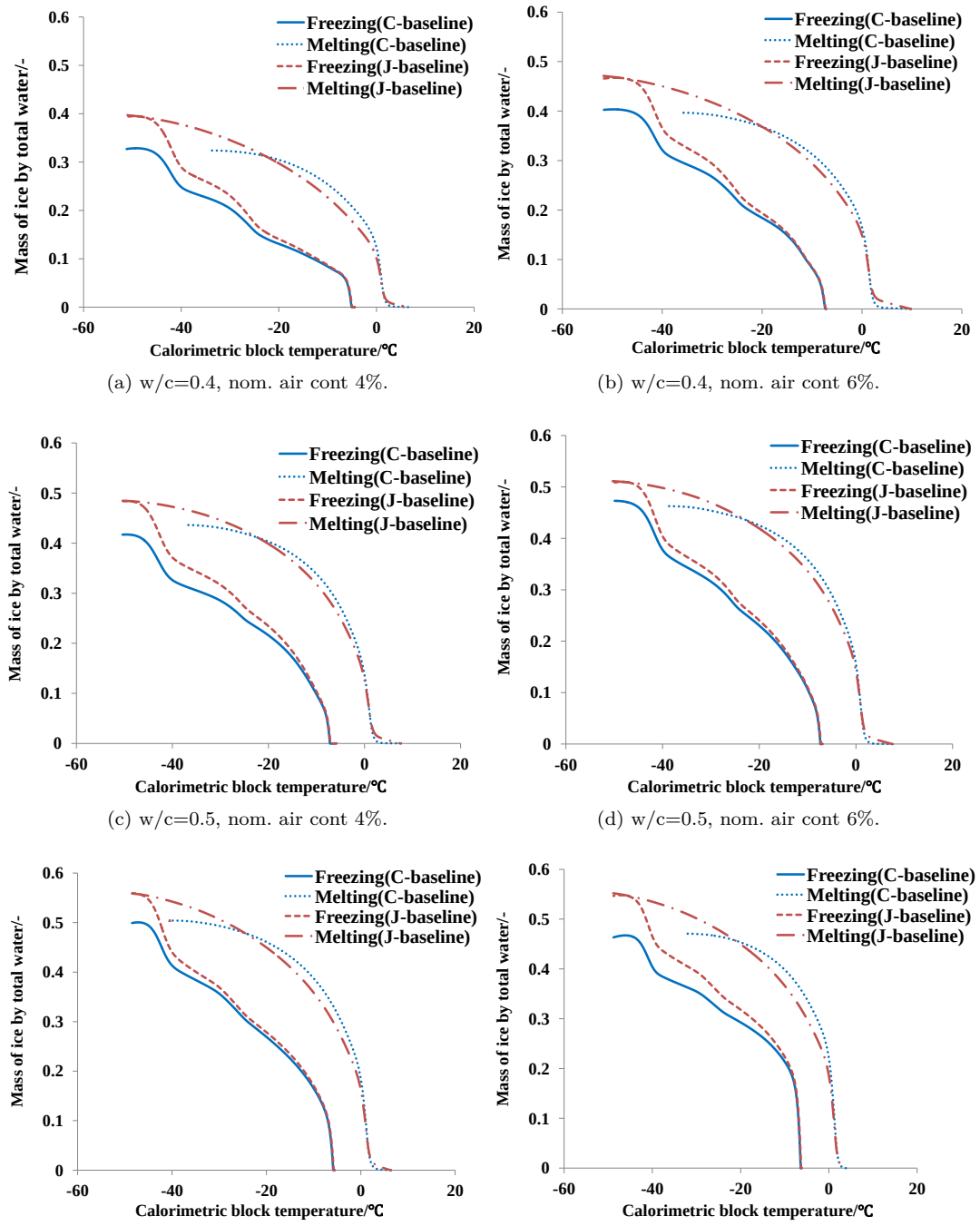

(a) w/c=0.4, nom. air cont 4%.

(b) w/c=0.4, nom. air cont 6%.

(c) w/c=0.5, nom. air cont 4%.

(d) w/c=0.5, nom. air cont 6%.

(e) w/c=0.6, nom. air cont 2%.

(f) w/c=0.6, nom. air cont 6%.

Fig. 3: Calculated mass of ice by total amount of water at different freezing and melting temperatures based on 'J-baseline' method and 'C-baseline' method. The heat of fusion and its temperature dependence for the confined water or ice is assumed as that presented in Eq.14. Capillary saturated samples are used in the testing.

For 'C-baseline' the calculation is based on the theoretical description of the phase changing behavior, it should give very close information to the true value under each temperature if the parameters adopted are correct. The accuracy can be further improved by considering the temperature dependent property of the heat capacity of water and ice combined with a careful experimental design by using a reference sample. However, it should also be noted that the temperature dependence of the heat capacity of water and ice under very low temperatures are not absolutely clear, especially for that of water. To measure the heat capacity of the water under 0 °C at atmospheric pressure, cares should be taken to keep the water under supercooled condition. This is not that easy to be achieved when the temperature is much lower compared to the freezing point of water. Under such cases, any fluctuations or uncertainties could initiate the crystallization of the liquid [44], making the direct measurement of the heat capacity extremely difficult. Different values of heat capacity of supercooled water were reviewed and reported in [44], which differ from Eq.3 especially when the temperature is under -20 °C. Since the reported values are also in a relatively wide range, it tends be of little meaning to study the impact of the different reported values of the heat capacity on the calculated ice content and thus the work is not conducted in this study.

While for the 'J-baseline', the calculated ice content could be very sensitive to the extrapolation procedure itself. In the extrapolation, one should choose several points to determine the initial slope on the heat-temperature curve and the starting point and the ending point for a process as well. Taking the melting process for example, the initial slope is not that straightforward to be found since the changing of slope at the whole low temperature range (till about -30 °C) is very small which is unlike the abrupt change of the initial slope for the freezing process, thus the choice of this slope is somewhat arbitrary. It is also not that straightforward to determine which temperature should be chosen as the starting point when the ice starts to melt. Assuming a lower temperature (compared with the true value) is chosen as the starting melting point, the slope of the b curve tends to be smaller and then the calculated baseline d will be higher than its true position (referring to Figure 1b). Consequently, the energy jump calculated accordingly will be overestimated. Since one of the principles for 'J-baseline' is to ensure the ice calculated in the freezing process is equal to that in the melting, the overestimated melting energy will also affect the calculated ice content in the freezing process. This could possibly explain partly the difference between the two methods as shown in Figure 3. Since it is difficult to judge the true temperature when ice just starts to melt, a temperature which is very close to the lowest ice-forming point is chosen as the starting melting point. However, according to 'C-baseline' method, the calculated starting melting temperatures of the ice are higher than the chosen points. Thus, the ice content calculated from the 'J-baseline' method is actually higher than that calculated from the 'C-baseline' method. If we move the starting point of the melting to the value as predicted by the 'C-baseline' method, it can be anticipated that both the freezing curve and the melting curve of the ice content will be in better agreement between these two methods. Fig.4 shows the results by doing the adjustment for sample C504 and C506, which does show that the ice curves are in better agreement, with still some little difference that might be due to other uncertainties, e.g. the heat capacities as aforementioned. In the verification experiment of 'J-baseline' by using water [20], which shows the estimated value varies about 2% (relative difference) compared with the true value, it is relatively very straightforward to choose the several points as needed for the extrapolation since all of the water will freeze/melt at one temperature giving very abrupt change of the slope in the accumulated energy curve. As for the case in this study, it is more complicated since the ice in concrete samples is continuously forming/melting under different temperatures. Nevertheless, an acceptable accuracy can be anticipated based on the 'J-baseline' method if special care is taken.

One advantage of the 'J-baseline' method is that the ice content calculation will not be affected by the uncertainties of the heat capacity of water and ice under very low temperatures as they are not inputs for the calculation. The calculated results can be expected in good accuracy provided a correct value of the heat of fusion (Section 4.2) is used. Additionally, the calculation will not be affected by the fluctuation of the cooling or heating rate in testing. While for the 'C-baseline' method, the uncertainties of the heat capacity of water and ice at very low temperatures could affect the calculated

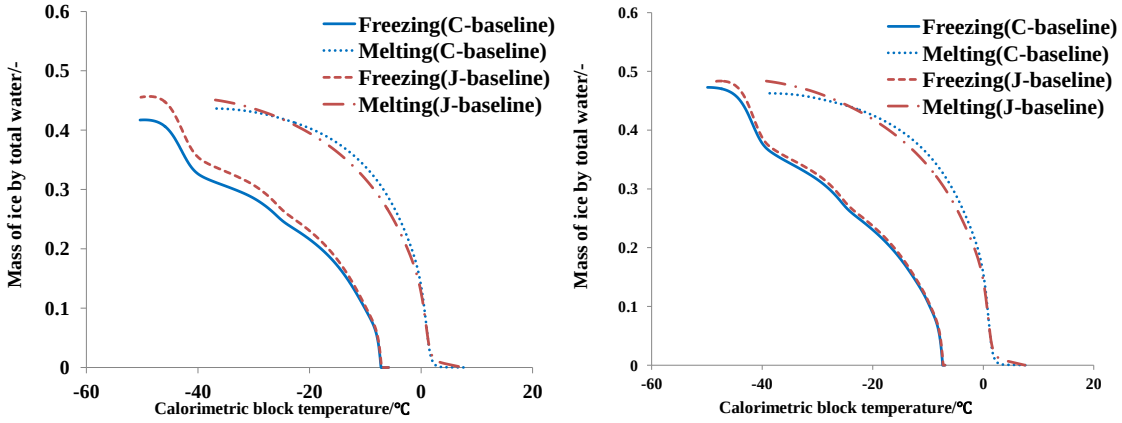

(a) w/c=0.5, nom. air cont 4%.

(b) w/c=0.5, nom. air cont 6%.

Fig. 4: Calculated mass of ice by total amount of water at different freezing and melting temperatures based on 'J-baseline' method with the starting melting point as predicted by'C-baseline' method. Compared with the results presented in Figure 3 (c and d), the ice curves are in better agreement.

results to a certain extent. Meanwhile, possible fluctuation of the cooling or heating rate should be taken into account. Bearing these in mind, actually these two methods can be used complementarily in practice.

4.2 Influence of the heat of fusion of confined water on the calculated ice content

As discussed already, different arguments exist regarding the heat of fusion for the water confined in pores. In order to study to what extend the value of the heat of fusion can affect the estimated ice content, comparison is performed by using the different values as presented in Section 3.2. The heat of fusion of bulk water which freezes/melts at 0 °C, $\triangle h = 334.1$ J g^{-1}, is also included in the comparison. In the following study, 'C-baseline' method is adopted in calculating the ice content. To simplify the discussion, the following abbreviations are used:

-HEBT is the heat of fusion for bulk water corrected for the depressed freezing or melting temperature of the pore water (i.e., Eq.14);

-HEB is the heat of fusion of the bulk water which freezes/melts at 0 °C (i.e., $\triangle h = 334.1$ J g^{-1});

-HEMC is the modified heat of fusion for cylindrical pores (i.e., Eq.17 for freezing and Eq.18 for melting);

-HEMS is the modified heat of fusion of water for spherical pores (i.e., Eq.17 for both freezing and melting).

In an attempt to verify which heat of fusion of the confined water is more reasonable, a comparison study is performed on the calorimetric measurements of a mono-sized model material named SilicaV432 using distilled water as the probe liquid. The experimental data and the details were presented in [4]. Two measurements on the same material but using different heating/cooling rate were conducted, measurements denoted as M1 (cooling and heating rate 1.2 °C h^{-1}) and M2 (cooling rate 3.3°C h^{-1} and heating rate 4.1 °C h^{-1}). The comparison results are presented in Figure 5 and Figure 6. It can be found that at higher temperatures, the ice curves show very good agreement while there are some differences at the low temperature range using the different values for the heat of fusion, especially in the freezing curves. The relative differences of the maximum ice content determined from

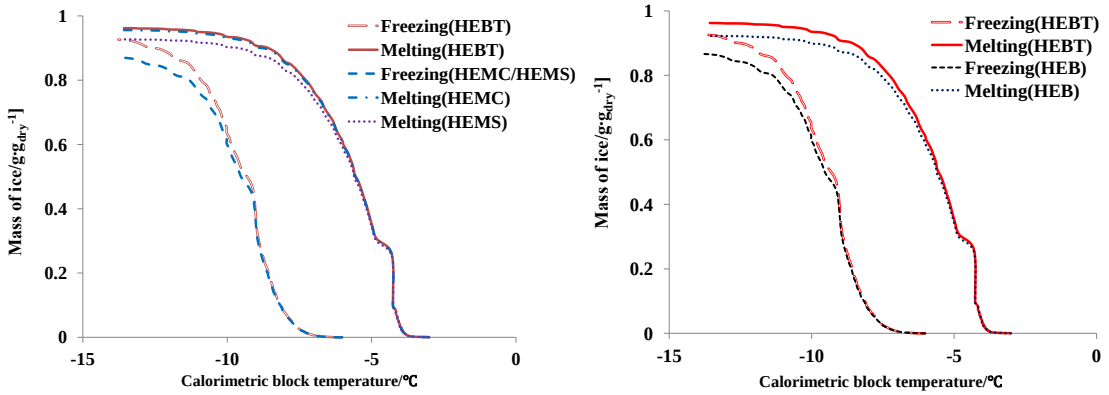

(a) (b)

Fig. 5: Amount of ice calculated using the 'C-baseline' method and different values of the heat of fusion for M1 (cooling and heating rate 1.2 °C h^{-1}), the amount of ice presented as the ice content per unit mass of dry model material. (a) comparison between the heat of fusion HEMC, HEMS and HEBT; (b) comparison between the heat of fusion HEB and HEBT.

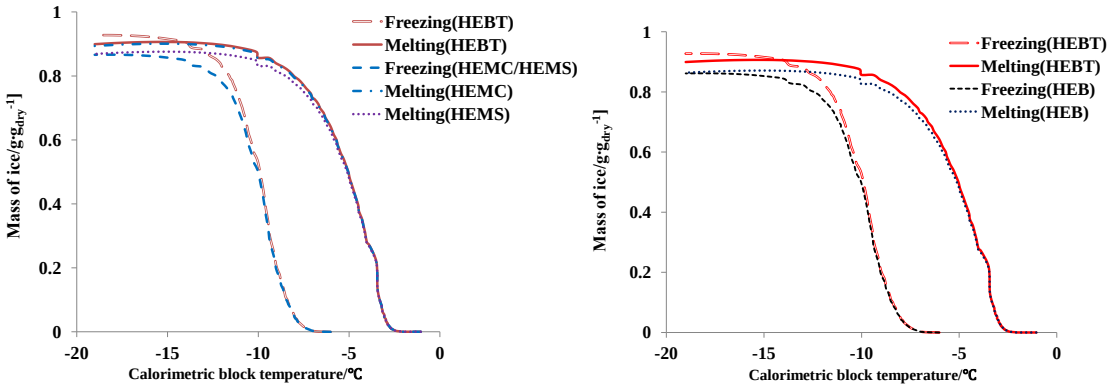

(a) (b)

Fig. 6: Amount of ice calculated using the 'C-baseline' method and different values of the heat of fusion for M2 (cooling rate 3.3 °C h^{-1} and heating rate 4.1 °C h^{-1}), the amount of ice presented as the ice content per unit mass of dry model material. (a) comparison between the heat of fusion HEMC, HEMS and HEBT; (b) comparison between the heat of fusion HEB and HEBT.

the freezing and melting process in one measurement cycle using the different heat of fusions are listed in Table 2.

According to Table 2, the relative differences between the calculated ice content from the freezing and melting process in one measurement cycle using different heat of fusions range from about -4% to -10% for M1 and about 3% to -0.4% for M2. It should be noted that the relative differences caused by the different heat of fusions are not significant, except that of HEMC for M1 (-9.76%). If the average of the ice content from the freezing and the melting is taken, the biggest relative difference for both M1 and M2 using different heat of fusions are about 5%. The very initial purpose of doing this comparison on the model material is to judge which heat of fusion makes most sense by studying the difference of the calculated ice content from the freezing and melting process in one measurement

Table 2: The relative differences of the maximum amount of ice per unit mass of dry model material calculated from the freezing and melting process in one measurement cycle using different values of the heat of fusion for the model material as presented in Figure 5 and Figure 6.

Measurement	Heat of fusion	Mass of ice (g g_{dry}^{-1})		Relative difference
		freezing	melting	(%)[a]
M1	HEBT	0.926	0.962	-3.89
	HEMC	0.871	0.956	-9.76
	HEMS	0.871	0.927	-6.43
	HEB	0.886	0.922	-4.06
M2	HEBT	0.927	0.899	3.02
	HEMC	0.866	0.894	-3.23
	HEMS	0.866	0.869	-0.35
	HEB	0.861	0.864	-0.35

Note: (a). the relative difference is calculated by: 100(column 3-column 4)/column 3.

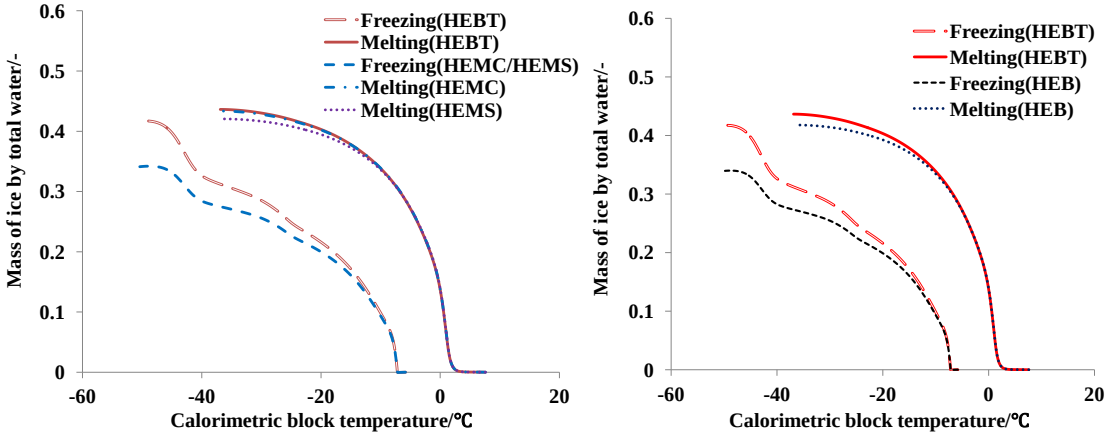

(a) (b)

Fig. 7: Ice content calculated using the 'C-baseline' method and different values of the heat of fusion for water saturated sample C504. (a) comparison between the heat of fusion HEMC, HEMS and HEB; (b) comparison between the heat of fusion HEB and HEBT.

cycle, which should be very close as the ice formed should be the ice melted in one cycle, and that of the ice content using different heat of fusions. However, it is difficult to judge by looking at the small differences as presented here. Thus, all the different values of the heat of fusion as discussed were applied to the concrete samples under study anyway.

The results for sample C504 is shown in Figure 7. According to Figure 7a, if the heat of fusion HEB is adopted, the ice content calculated from the freezing curve will be higher than that calculated using the modified heat of fusion HEMC. The difference is small in the high temperature range, but increases as the freezing temperature keeps decreasing. The relative difference is about 23% when the temperature is about -50 °C. For the melting curve, the calculated ice content based on HEMC and HEB are in quite good agreement. For the same freezing and melting cycle, the maximum ice content determined from the freezing and the melting process, differs significantly based on HEMC, the relative difference being as much as about 27%, see Figure 7a. While the ice content calculated based on HEBT in the same freezing and melting cycle only varies about 2%. The ice contents determined from the freezing process based on HEMC and HEMS are the same, since Eq.17 is used for the both cases. For

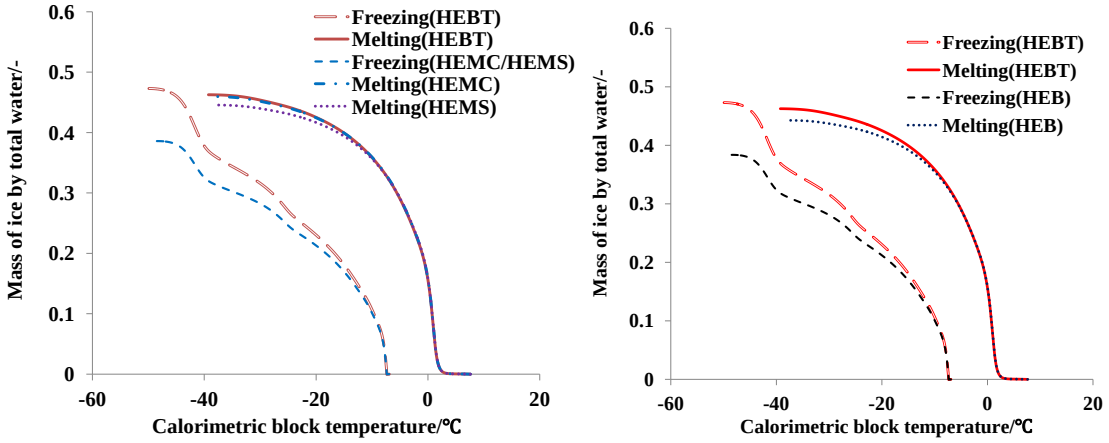

Fig. 8: Ice content calculated using the 'C-baseline' method and different values of the heat of fusion for water saturated sample C506. (a) comparison between the heat of fusion HEMC, HEMS and HEBT; (b) comparison between the heat of fusion HEB and HEBT.

the melting curve, the ice content deduced from HEMS is in relatively good agreement with the value calculated based on HEMC, though at the low temperature range the value based on HEMS is smaller than that based on HEMC, showing a difference of about 3% at the lowest melting temperature for the sample (see Figure 7a). That is, it can be concluded that the pore shape assumptions will not significantly affect the estimated ice content for a concrete sample if the modified heat of fusion is adopted.

The comparison between the ice content based on heat of fusion HEBT and HEB demonstrates some difference, as shown in Figure 7b. In the freezing process, the maximum ice content calculated based on HEBT differs from that based on HEB, the difference being increasing as the temperature decreases leading to a largest relative difference about 28% at the lowest ice forming temperature. While for the melting, the two curves are in certain agreement especially at the high temperature range, though a difference of 4% is found for the maximum ice content. For the same cycle of freezing and melting, the maximum ice content based on HEB differs about 23%, see Figure 7b. This is in agreement with the findings discussed in [64], which show a difference about 20% where a constant heat of fusion, i.e., HEB in our discussion, was used in the calculation.

In general, as for the calculated ice content based on HEBT and HEMC, large difference is shown for the freezing process while a relatively good agreement can be found for the melting process. If the modified heat of fusion HEMC or HEMS is used, the pore shape assumptions will not have a major effect on the estimated ice content for a concrete sample. A difference of about 20% will be observed if the heat of fusion for the normal bulk water or ice which freezes/melts at 0 °C is adopted in the calculation of the ice content between the freezing and melting process in one freezing and melting cycle.

The same trends as discussed before can be found for other samples. Figure 8 shows the comparison for the sample C506 and Figure 9 for C602. The relative difference of the maximum ice content determined based on HEBT and HEMC can be found as about 23% and 20% in freezing for sample C506 and C602 respectively; while for melting, they are in very good agreement with the largest variation of less than 2%. The comparison between the values of the maximum ice content based on HEBT and HEB shows a relative difference of about 23% and 21% in the freezing and about 5% and 4% in the melting for sample C506 and C602 respectively.

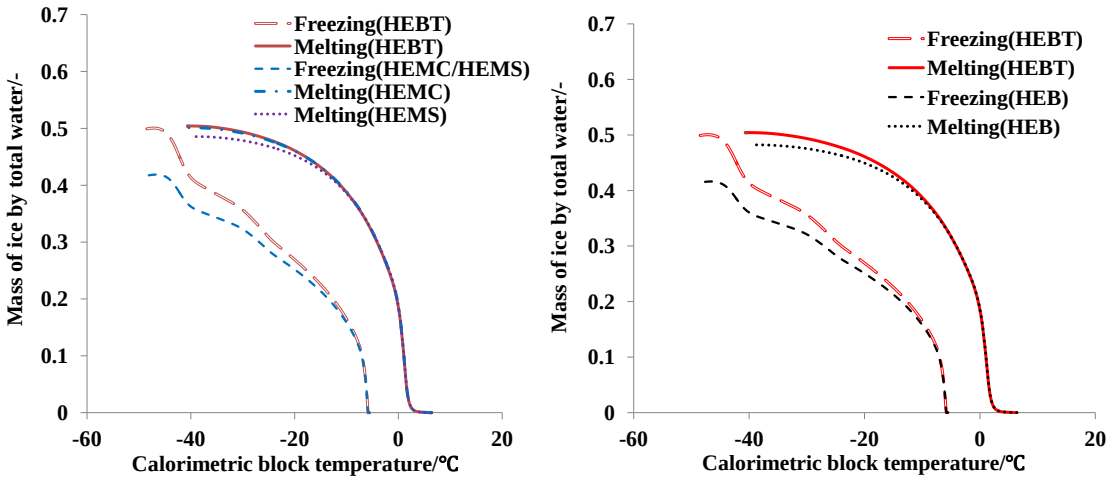

(a) (b)

Fig. 9: Ice content calculated using the 'C-baseline' method and different values of the heat of fusion for water saturated sample C602. (a) comparison between the heat of fusion HEMC, HEMS and HEBT; (b) comparison between the heat of fusion HEB and HEBT.

Based on the above discussion, certain difference is found for the calculated ice content for the concrete samples if different values of the heat of fusion of the confined water are adopted. As demonstrated already, the heat of fusion may be related to the pore shape of the sample under testing. However, it is often not that straightforward to define the pore shape in a concrete sample due to its complexity. Moreover, since we have no direct information with respect to the pore volume of the concrete samples tested, it is not possible to judge which value for the heat of fusion and its temperature dependence is most reasonable by comparing the measured pore volume and the real pore volume. During the discussion, the difference of the ice content calculated for the freezing and melting process in one freezing and melting cycle is compared from time to time. Actually, this could be a very practical criterion to judge which value of the heat of fusion and its temperature dependence makes more sense, since the maximum ice content formed in the freezing process should be equal to that melted in the melting process in one freezing and melting cycle. Accordingly, if this criterion is adopted, it seems that it makes more sense to use the heat of fusion of bulk water but corrected for the depressed freezing/melting point of the pore water (HEBT) for the analysis.

It should be mentioned that the difference of the calculated ice contents for the mono-size model material SilicaV432 are much smaller by adopting different values of the heat of fusion of the confined water, as presented before. Compared with the mono-sized model material, the pores inside of concrete are much more widely distributed. Thus, the freezing/melting of the pore water in concrete covers a long range of temperatures. Then the impact of the heat of fusions becomes pronounced on the calculated ice content. While the freezing/melting of the pore water in the mono-sized material only covers a small temperature range, the impact of the heat of fusions on the calculated ice content may be not that pronounced, as observed in Figure 5 and Figure 6. In this sense, it may be more appropriate to study a model material with more than one pore size (or simply a mixture of two or more model materials with different pore sizes) in order to stringently validate which heat of fusion should be adopted in this context of calculation.

In this study, the heat of fusion of pure water is used to calculate the ice content for simplicity. One may argue that the difference of the calculated maximum ice content in the freezing and melting process of one cycle might be related to the ions in the pore solution of the concrete samples, since

the heat of fusion of pore solution might differ from that of pure water. Then, it is not applicable to use the heat of fusion of pure water in the calculation. It has been noted that some authors [12, 18] suggested that the concrete pore solution could become dilute during the long time curing in water and the pore solution can be approximated to saturated calcium hydroxide solution (the concentration is $\sim$2 g L^{-1}) [18]. That is, the studied concrete pore solution in our case might be very dilute. On the other hand, there are several types of ionic species in the pore solution of a concrete sample [40, 65] and the effect of different ions on the heat of fusion of the water is also different [66]. As described in [66], there are basically two different types of ions, one of which would cause the increase of the heat of fusion of water and the other has exactly the opposite effect. Due to the complexity of the ions in the rather dilute pore solution, the heat of fusion of the pure water consequently might not be a bad approximation for the pore solution in the context of ice content predication. With the lack of further knowledge about the heat of fusion of the pore solution, the heat of fusion of pure water is used. Obviously, further study is needed to clarify related issues. A possible alternative in this context is to use NMR cryoporometry [67] as a complementary method, which follows the same concept of freezing and melting but the ice content is determined quite differently. By comparing the ice content under different freezing/melting temperatures using the two different methods, it could be possible to judge if a certain choice of the temperature dependent function describing the heat of fusion is more reasonable than others. Further discussion in this regard falls outside the scope of this paper.

5 Conclusions

Low temperature (micro-)calorimetry (LTC) has been used to determine the ice content in concrete at different temperatures by carefully studying the freezing /melting behavior of the confined water in the pores. LTC is also widely used to investigate the porosity at nanometric level. The present study focuses on exploring the important factors influencing the analysis of LTC data with the purpose of improving the accuracy of determining the ice content.

The importance of the baseline determination for the calculation of ice content is illustrated. Two different methods of generating the baseline were discussed. The 'J-baseline' method is a recently proposed method based on extrapolation by using the accumulated heat curves measured in the freezing and the melting process. The 'C-baseline' considers the heat capacity of both water and ice and the phase changing behavior under the different testing temperatures. Both methods can be used for baseline and ice content calculation if due attention is paid. Results obtained by the 'J-baseline' method are not affected by the uncertainties of the heat capacity of water and ice under very low temperatures and the possible fluctuations of the cooling and heating rate during testing; while the 'C-baseline' can deliver more accurate result due to its more stringent theoretical basis, provided the corrected thermodynamic parameters are used. These two methods can be used complementarily in practice.

The influence of the different values of the heat of fusion commonly adopted in literature on the calculated ice content is investigated. For the studied concrete samples, the relative difference of the maximum ice content determined from one freezing and melting cycle can differ up to 27% due to using different values of the heat of fusion. Using the heat of fusion of bulk water but corrected for the depressed freezing/melting temperature of the pore water results in the smallest difference between the maximum ice content calculated from the measured heat flow during freezing and melting in one cycle.

Acknowledgment

The research leading to these results has received funding from the European Union Seventh Framework Programme (FP7/2007-2013) under grant agreement 264448.

Appendix A. Supplementary material

Supplementary data associated with this article can be found, in the online version, at (DOI added later by the editor).

References

1. A.M. Neville. *Properties of concrete*. Prentice Hall, 4th edition edition, 1995.
2. S. Diamond. Aspects of concrete porosity revisited. *Cement and Concrete Research*, 29(8):1181–1188, 1999.
3. M. Pigeon and R. Pleau. *Durability of concrete in cold climates*. Number 4. Taylor & Francis, 1995.
4. A.M. Kjeldsen and M.R. Geiker. On the interpretation of low temperature calorimetry data. *Materials and Structures*, 41(1):213–224, 2008.
5. W. Kuhn, E. Peterli, and H. Majer. Freezing point depression of gels produced by high polymer network. *Journal of Polymer Science*, 16(82):539–548, 1955.
6. J.R. Blachere and J.E. Young. The freezing point of water in porous glass. *Journal of the American Ceramic Society*, 55(6):306–308, 1972.
7. J. Riikonen, J. Salonen, and V.P. Lehto. Utilising thermoporometry to obtain new insights into nanostructured materials (review part 1). *Journal of Thermal Analysis and Calorimetry*, 105: 811–821, 2011.
8. J. Riikonen, J. Salonen, and V.P. Lehto. Utilising thermoporometry to obtain new insights into nanostructured materials (review part 2). *Journal of Thermal Analysis and Calorimetry*, 105: 823–830, 2011.
9. D. Majda, W. Makowski, and M. Mańko. Pore size distribution of micelle-templated silicas studied by thermoporosimetry using water and n-heptane. *Journal of Thermal Analysis and Calorimetry*, 109(2):663–669, 2012.
10. E. Illeková, M. Miklošovičová, O. Šauša, and D. Berek. Solidification and melting of cetane confined in the nanopores of silica gel. *Journal of Thermal Analysis and Calorimetry*, 108(2): 497–503, 2012.
11. P.J. Williams. Properties and behavior of freezing soils. Technical Report 72, Norwegian Geotechnical Institute, Oslo,Norway, 1961.
12. G. Fagerlund. Determination of pore-size distribution from freezing-point depression. *Materials and Structures*, 6(3):215–225, 1973.
13. M. Brun, A. Lallemand, J.F. Quinson, and C. Eyraud. A new method for the simultaneous determination of the size and shape of pores: the thermoporometry. *Thermochimica Acta*, 21(1): 59–88, 1977.
14. J.W.P. Schmelzer, editor. *Nucleation Theory and Applications*. WILEY-VCH, 2005.
15. G.W. Scherer. Freezing gels. *Journal of non-crystalline solids*, 155(1):1–25, 1993.
16. M.J. Setzer. Micro-ice-lens formation in porous solid. *Journal of Colloid and Interface Science*, 243(1):193–201, 2001.
17. J.P. Kaufmann. Experimental identification of ice formation in small concrete pores. *Cement and Concrete Research*, 34(8):1421–1427, 2004.
18. Z. Sun and G.W. Scherer. Pore size and shape in mortar by thermoporometry. *Cement and Concrete Research*, 40(5):740–751, 2010.
19. R. Defay, I. Prigogine, A. Bellemans, and D.H Everett. *Surface tension and adsorption*. Longmans London, 1966.
20. K. Fridh. *Internal frost damage in concrete–experimental studies of destruction mechanisms*. PhD thesis, Division of Building Materials, Lund Institute of Technology, 2005.

21. M. Wu, B. Johannesson, and M. Geiker. Impact of sample saturation on the detected porosity of hardened concrete using low temperature calorimetry. Cement and Concrete Composites, submitted for publication.
22. F. Radjy, E.J. Sellevoid, and C.W. Richards. Effect of freezing on the dynamic mechanical response of hardened cement paste down to -60 °C. *Cement and Concrete Research*, 2(6):697–715, 1972.
23. F. Radjy and E.J. Sellevold. Internal friction peaks due to adsorbed and capillary water in microporous substances. *Nature*, 241(111):133–135, 1973.
24. C. Le Sage de Fontenay. *Ice formation in hardened cement paste (in Danish)*. PhD thesis, Building Materials Laboratory, Technical University of Denmark, 1982.
25. D.H. Bager. *Ice Formation in Hardened Cement Paste*. PhD thesis, Building Materials Laboratory, Technical University of Denmark, 1984.
26. D.H. Bager and E.J. Sellevold. Ice formation in hardened cement paste, Part I–room temperature cured pastes with variable moisture contents. *Cement and Concrete Research*, 16(5):709–720, 1986.
27. D.H. Bager and E.J. Sellevold. Ice formation in hardened cement paste, Part II-drying and resaturation on room temperature cured pastes. *Cement and Concrete Research*, 16(6):835–844, 1986.
28. D.H. Bager and E.J. Sellevold. Ice formation in hardened cement paste, Part III-slow resaturation of room temperature cured pastes. *Cement and Concrete Research*, 17(1):1–11, 1987.
29. J. Villadsen. Pore structure in cement based materials. Technical Report 277, Building Materials Laboratory, Technical University, Denmark, 1992.
30. S. Jacobsen and E.J. Sellevold. Frost/salt scaling and ice formation of concrete: effect of curing temperature and silica fume on normal and high strength concrete. In J. Marchand, M. Pigeon, and M. Setzer, editors, *RILEM PROCEEDINGS 30. FREEZE-THAW DURABILITY OF CONCRETE*, pages 93–105, 1997.
31. E.W. Hansen, H.C. Gran, and E.J. Sellevold. Heat of fusion and surface tension of solids confined in porous materials derived from a combined use of NMR and calorimetry. *The Journal of Physical Chemistry B*, 101(35):7027–7032, 1997.
32. F. Radjy, E.J. Sellevold, and K.K. Hansen. Isoteric vapor pressure–temperature data for water sorption in hardened cement paste: enthalpy, entropy and sorption isotherms at different temperatures. Technical Report BYG-DTU R057, Technical University of Denmark(DTU), Lyngby, Denmark, 2003.
33. B. Johannesson. Dimensional and ice content changes of hardened concrete at different freezing and thawing temperatures. *Cement and Concrete Composites*, 32(1):73–83, 2010.
34. B. Johannesson and G. Fagerlund. Concrete for the storage of liquid petroleum gas–freeze/thaw phenomena and durability at freezing to -50 °C. Report TVBM– 7174, Division of Building Materials, Lund Institute of Technology, 2003.
35. G. Fagerlund and B. Johannesson. Concrete for the storage of liquid petroleum gas, Part II: influence of very high moisture contents and extremely low temperatures, -196 °C. Report TVBM - 1851, Division of Building Materials, Lund Institute of Technology, 2005.
36. M.R. Landry. Thermoporometry by differential scanning calorimetry: experimental considerations and applications. *Thermochimica Acta*, 433(1-2):27–50, 2005.
37. G. Fagerlund. Studies of the scaling, the water uptake and the dilation of specimens exposed to freezing and thawing in NaCl solution. In *Proceedings of RILEM committee 117 DC Freezing/thaw and de-icing resistance of concrete*, pages 37–66, Swden, 1991.
38. R.A. Helmuth. Capillary size-restrictions on ice-formation in hardened portland cement-pastes. In *Proceedings of 4th Symposium on Chemistry of Cement*, volume 2, Washington DC, 1960.
39. TC Powers. Physical properties of cement paste. In *Proc. Fourth Int. Symp. on the Chemistry of Cement, Washington, DC*, 1960.
40. H.F.W. Taylor. *Cement chemistry*. Thomas Telford, London, 2nd edition, 1997.

41. B. Lothenbach and F. Winnefeld. Thermodynamic modelling of the hydration of portland cement. *Cement and Concrete Research*, 36(2):209–226, 2006.
42. C. D. Hodgman, R. C. Weast, and S. M. Selby, editors. *Handbook of Chemistry and Physics*. The Chemical Rubber Co., Cleveland (Ohio)., 45 edition, 1965.
43. D. Gray, editor. *American Institute of Physics Handbook*. McGraw- Hill, New York, 2nd edition, 1963.
44. D.M. Murphy and T. Koop. Review of the vapour pressures of ice and supercooled water for atmospheric applications. *Quarterly Journal of the Royal Meteorological Society*, 131(608):1539–1565, 2005.
45. M. Wu. Imapct of cooling/heating rate drifting or fluctutaion on the caculated ice content by low temperature calorimetry. Study Report, Building Materials Laboratory, Technical University of Denmark, 2011.
46. K. Ishikiriyama, M. Todoki, K.H. Min, S. Yonemori, and M. Noshiro. Pore size distribution measurements for microporous glass using differential scanning calorimetry. *Journal of Thermal Analysis and Calorimetry*, 46(3-4):1177–1189, 1996.
47. K. Ishikiriyama, M. Todoki, and K. Motomura. Pore size distribution (PSD) measurements of silica gels by means of differential scanning calorimetry I. optimization for determination of PSD. *Journal of Colloid and Interface Science*, 171(1):92–102, 1995.
48. K. Ishikiriyama and M. Todoki. Evaluation of water in silica pores using differential scanning calorimetry. *Thermochimica Acta*, 256(2):213–226, 1995.
49. K. Ishikiriyama and M. Todoki. Pore size distribution measurements of silica gels by means of differential scanning calorimetry II. thermoporosimetry. *Journal of Colloid and Interface Science*, 171(1):103–111, 1995.
50. M. Brun, A. Lallemand, J.F. Quinson, and C. Eyraud. Changement d'état liquid–solide dans les milieux poreux. II. Étude théorique de la solidification d'un condensate capillaire (liquid–solid change of state in porous media. II. Theoretical study of the solidification of a capillary condensate). *J.Chim.Phys.*, 6:979–989, 1973.
51. M. Randall. *International Critical Tables V–VII*. McGraw–Hill, New York, 2nd edition, 1930.
52. C.S. Chen. Systematic calculation of thermodynamic properties of an ice-water system at sub-freezing temperatures. *Transactions of the ASAE*, 31(5):1602–1606, 1988.
53. T. Yamamoto, A. Endo, Y. Inagi, T. Ohmori, and M. Nakaiwa. Evaluation of thermoporometry for characterization of mesoporous materials. *Journal of Colloid and Interface Science*, 284(2): 614–620, 2005.
54. T. Yamamoto, S.R. Mukai, K. Nitta, H. Tamon, A. Endo, T. Ohmori, and M. Nakaiwa. Evaluation of porous structure of resorcinol-formaldehyde hydrogels by thermoporometry. *Thermochimica acta*, 439(1):74–79, 2005.
55. E. Sellevold and D. Bager. Some implications of calorimetric ice formation results for frost reistance testing of concrete. *in Beton og Frost, Dansk Betonforening*, 22:47–74, 1985.
56. J.F. Quinson, M. Astier, and M. Brun. Determination of surface areas by thermoporometry. *Applied Catalysis*, 30(1):123–130, 1987.
57. J.F. Quinson and M. Brun. Progress in thermoporometry. *K. K. Unger, J. Rouquerol, K. S.W Sing and H. Kral (eds): Characterization of Porous Solids, Elsevier, Amsterdam*, page 307, 1988.
58. M. Brun, J.F. Quinson, and L. Benoist. Determination of pore size distribution by SETARAM DSC 101 (thermoporometry). *Thermochimica Acta*, 49(1):49–52, 1981.
59. C. Eyraud, J.F. Quinson, and M. Brun. The role of thermoporometry in the study of porous solids. *Studies in Surface Science and Catalysis*, 39:295–305, 1988.
60. C.J.G. Van der Grift, A.Q.M. Boon, A.J.W. Van Veldhuizen, H.G.J. Trommar, J.W. Geus, J.F. Quinson, and M. Brun. Preparation and characterization of porous silica spheres containing a copper (oxide) catalyst. *Applied Catalysis*, 65(2):225–239, 1990.
61. M. Stöcker. *Thermoporometry, in Handbook of Porous Solids*. Wiley-VCH Verlag GmbH, Weinheim, Germany, 2008.

62. J.N. Hay and P.R. Laity. Observations of water migration during thermoporometry studies of cellulose films. *Polymer*, 41(16):6171–6180, 2000.
63. A. Książczak, A. Radomski, and T. Zielenkiewicz. Nitrocellulose porosity-thermoporometry. *Journal of Thermal Analysis and Calorimetry*, 74(2):559–568, 2003.
64. Z. Sun and G.W. Scherer. Effect of air voids on salt scaling and internal freezing. *Cement and Concrete Research*, 40(2):260–270, 2010.
65. B. Lothenbach. Thermodynamic equilibrium calculations in cementitious systems. *Materials and Structures*, 43(10):1413–1433, 2010.
66. G.M. Mrevlishvili and P.L. Privalov. Calorimetric study of the melting of frozen aqueous solutions of electrolytes. *Journal of Structural Chemistry*, 9(1):5–7, 1968.
67. J. Mitchell, J.B.W. Webber, and J.H. Strange. Nuclear magnetic resonance cryoporometry. *Physics Reports*, 461(1):1–36, 2008.

Supplementary material

November 16, 2013

Article title: Determination of ice content in hardened concrete by low temperature calorimetry: influence of baseline calculation and heat of fusion of confined water.

Journal name: Journal of Thermal Analysis and Calorimetry.

Authors: Min Wu[1*], Björn Johannesson[1], Mette Geiker[2].

Address: 1. Department of Civil Engineering, Building 118, Technical University of Denmark, 2800 Lyngby, Denmark; 2. Department of Structural Engineering, Norwegian University of Science and Technology, Trondheim, Norway.

[*]**E-mail:** miwu@byg.dtu.dk.

1. Figure 1 shows the Calvet-type scanning calorimeter (SETARAM) used for this investigation.

Figure 1: Top of the SETARAM scanning calorimeter showing the liquid nitrogen supply tube and the reference and sample chamber (after [1]).

2. The comparison between the modified (adopted in this study) and the original "J-method" [1] for baseline and ice content calculation is shown in Figure 2. The comparison between the modified (adopted in this study) and the original "C-method" [2] for baseline and ice content calculation is shown in Figure 3.

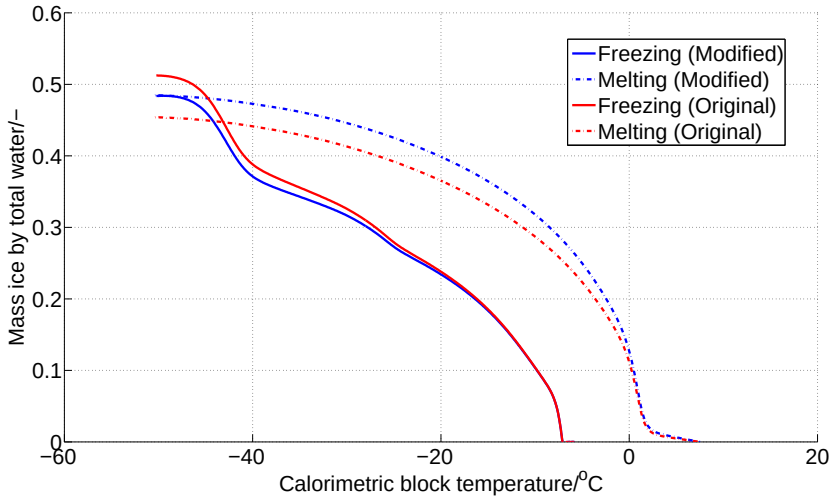

(a) w/c=0.5, nom. air cont 4%.

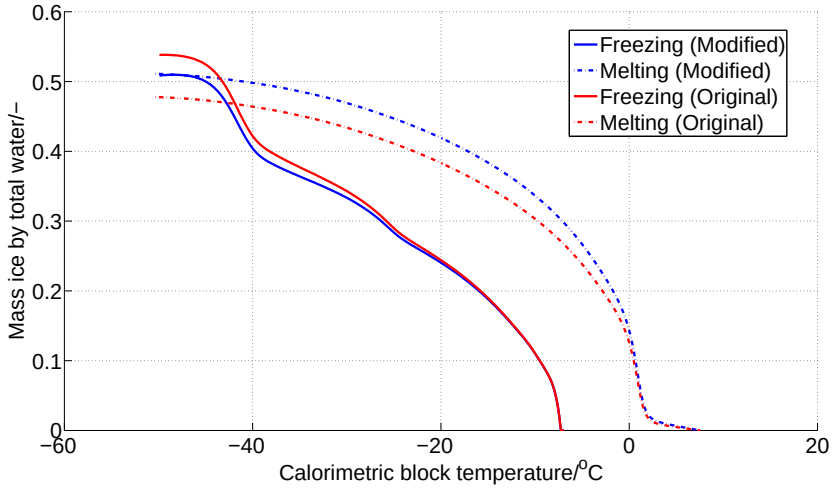

(b) w/c=0.5, nom. air cont 6%.

Figure 2: The comparison between the modified (adopted in this study) and the original "J-method" for baseline and ice content calculation for two capillary saturated concrete samples. The heat of fusion and its temperature dependence for the confined water or ice is assumed as HEBT.

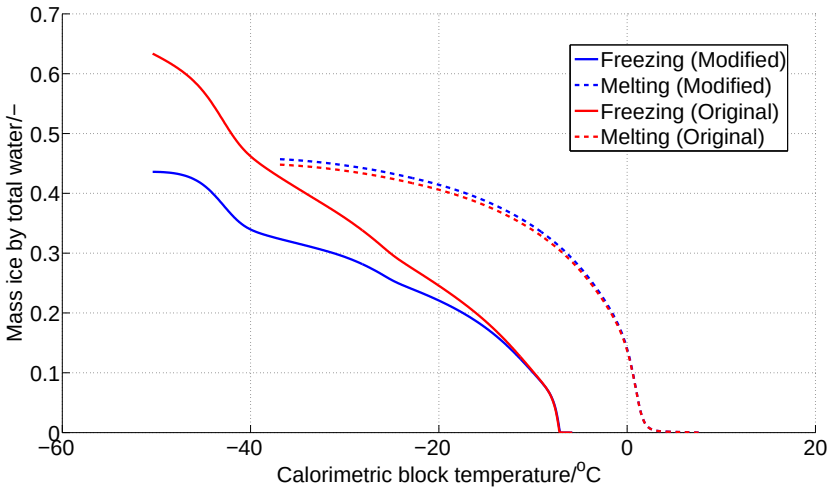

(a) w/c=0.5, nom. air cont 4%.

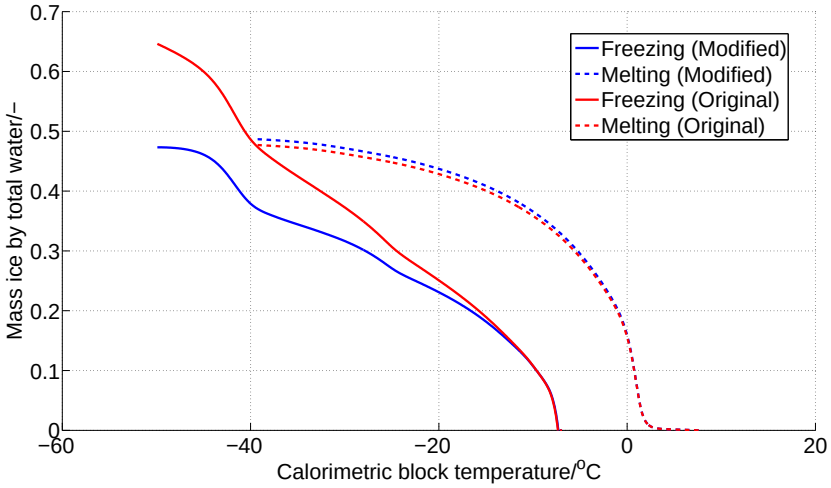

(b) w/c=0.5, nom. air cont 6%.

Figure 3: The comparison between the modified (adopted in this study) and the original "C-method" for baseline and ice content calculation for two capillary saturated concrete samples. The heat of fusion and its temperature dependence for the confined water or ice is assumed as HEBT. In the original method, the drifting of the cooling/heating rate is not taken into account.

References

[1] B. Johannesson. Dimensional and ice content changes of hardened concrete at different freezing and thawing temperatures. *Cement and Concrete Composites*, 32(1):73–83, 2010.

[2] Z. Sun and G.W. Scherer. Pore size and shape in mortar by thermoporometry. *Cement and Concrete Research*, 40(5):740–751, 2010.